New Journal of Physics
The open-access journal for physics

Continuous variable multipartite entanglement and optical implementations of quantum communication networks

Yimin Lian, Changde Xie and Kunchi Peng
State Key Laboratory of Quantum Optics and Quantum Optics Devices, Institute of Opto-Electronics, Shanxi University, Taiyuan 030006, People's Republic of China
E-mail: changde@sxu.edu.cn

New Journal of Physics **9** (2007) 314
Received 30 March 2007
Published 7 September 2007
Online at http://www.njp.org/
doi:10.1088/1367-2630/9/9/314

Abstract. A variety of optical quantum information networks based on the multipartite entanglement of amplitude and phase quadratures of an electromagnetic field have been proposed and experimentally realized in recent years. The multipartite entanglement of optical continuous variables provides flexible and reliable quantum resources for developing unconditional quantum information networks. In this paper, we review the generation schemes of the multipartite entangled states of optical continuous quantum variables and some applications in the quantum communication networks with emphasis on the experimental implementations.

Contents

PII: S1367-2630(07)47419-5

1. Introduction

Multipartite entanglement is one of the most fundamental and important quantum resources for developing quantum communication networks. To characterize the entanglement of states shared by many parties Coffman, Kundu and Wootters (CKW) discovered so-called 'monogamy inequalities', constraining the maximal entanglement distributed among different internal partitions of a multiparty system [1]. Then Adesso and Illuminati introduced a measure of entanglement for continuous-variable (cv) systems to quantify the distributed entanglement in multimode, multipartite Gaussian states and proved that the cv entanglement satisfies the CKW monogamy inequality in all three-mode Gaussian states, and in all fully symmetric N-mode Gaussian states, for arbitrary N [2]. A complete quantitative theory of multipartite entanglement based on the monogamy of entanglement has been discussed in detail in [2, 3]. Originally, the quantum information was developed in discrete variable (dv) systems and then was extended to the cv setting. In recent years, cv quantum information has attracted extensive interest due to the high efficiency in the generation, manipulation and detection of optical cv states [4]. The successful realization of unconditional quantum teleportation [5], dense coding [6] and entanglement swapping [7] based on cv Einstein–Podolsky–Rosen (EPR) entangled states of optical fields promoted investigations into the generation and application of cv multipartite entangled states. van Loock and Braunstein [8] proposed a scheme to produce cv multipartite entanglement using single-mode squeezed states and linear optics and designed a quantum teleportation network for its application in 2000. The necessary conditions and the experimental criteria to detect genuine multipartite cv entanglement were derived by van Loock and Furusawa [9]. Successively, cv tripartite entangled states of optical fields were experimentally obtained and applied in controlled dense coding quantum communication, tripartite quantum state sharing (QSS) and a quantum teleportation network by three groups in China, Japan and Australia, respectively [10]–[13]. The equivalence between entanglement and the optimal fidelity of cv teleportation was theoretically proven [14]. It was shown in [14] that a non-classical optimal fidelity of N-user teleportation networks is necessary and sufficient for N-party entangled Gaussian resources and thus allows for the definition of the entanglement of teleportation, an operative estimator of multipartite entanglement in a cv system.

The aim of writing this paper is not to present a comprehensive review on cv quantum entanglement and communication. We would like to emphasize the experimental implementations of cv multipartite entanglement generation with quantum optical systems and its applications in quantum communication networks. In this paper, we will introduce the experimental schemes for generating cv multipartite entanglement of optical fields in section 2 firstly, in which we concentrate on three-mode Gaussian states. Then two experimental systems for two applications of tripartite cv entangled states in quantum communication networks will be briefly described in sections 3 and 4, respectively. Finally, a short prospection is given in section 5.

2. Generation of multipartite cv entangled states

Quantum entanglement shared by more than two parties is named multipartite entanglement. Very recently, an extended study on how to produce, detect and employ multipartite entanglement for quantum communication with three-mode Gaussian states in an optical context was analyzed in depth and a simple procedure to produce pure three-mode Gaussian states

with arbitrary entanglement structure was introduced [15]. A mathematical framework for the characterization of separability and entanglement of formation of general bipartite states has been developed by Audenert *et al* [16]. In the quantum optical realm, we consider the multipartite entangled states consisting of the multipart multi-mode with one mode per party, and the amplitude and phase quadratures of electromagnetic modes are used for the continuous quantum variables. The sufficient conditions for verifying unambiguously the presence of genuine multipartite entanglement among optical modes were given in terms of the variances of the amplitude and phase quadrature combinations in [9]. A set of inequalities containing the conjugate variables of all modes provides reliable criteria for the verification of the cv multipartite entanglement. The violations of the inequalities are sufficient for genuine multipartite entanglement. Based on these inequalities, we can check the full inseparability of an optical state by the experimentally measurable variances of the quadrature combinations. For example, we consider the cv analogue [8, 17] of the Greenberger–Horne–Zeilinger (GHZ) state [18] involving three entangled modes. In this case, the inequalities are written as follows [9].

$$\begin{aligned} &\text{I.} \quad \left\langle \delta^2(\hat{x}_1 - \hat{x}_2) \right\rangle + \left\langle \delta^2(\hat{y}_1 + \hat{y}_2 + g_3\hat{y}_3) \right\rangle \geqslant 1, \\ &\text{II.} \quad \left\langle \delta^2(\hat{x}_2 - \hat{x}_3) \right\rangle + \left\langle \delta^2(g_1\hat{y}_1 + \hat{y}_2 + \hat{y}_3) \right\rangle \geqslant 1, \\ &\text{III.} \quad \left\langle \delta^2(\hat{x}_1 - \hat{x}_3) \right\rangle + \left\langle \delta^2(\hat{y}_1 + g_2\hat{y}_2 + \hat{y}_3) \right\rangle \geqslant 1, \end{aligned} \tag{1}$$

where $\hat{x}_i$ and $\hat{y}_i$ $(i = 1, 2, 3)$ stand for the amplitude and phase quadratures of the three modes, respectively. The g_i are arbitrary real parameters named the gain parameters. The optimum gains g_i^{opt} are adjusted to minimize the left-hand sides of the inequalities in equations (1). It has been proved in [9] that the violation of any two of the three inequalities in equations (1) is sufficient for genuine tripartite three-mode entanglement.

van Loock and Braunstein [8] firstly proposed a scheme to produce multipartite entanglement for cv of an optical field with the superposition of independently squeezed states and theoretically proved that even one single-mode squeezed state is sufficient for yielding a truly multipartite entangled state through the linearly optical transformation. Later, we designed a system generating a cv tripartite entangled state with a bright two-mode squeezed state from a non-degenerate optical parametric amplifier (NOPA) operating at deamplification [19]. The two-mode squeezed state generated from the NOPA consists of a signal mode $(\hat{x}_s, \hat{y}_s)$ and an idler mode $(\hat{x}_l, \hat{y}_l)$ with orthogonal polarizations and identical frequency. The amplitude and phase quadratures of the signal and idler modes are anticorrelated and correlated respectively, i.e. both variances of the sum of amplitude quadratures $\langle \delta^2(\hat{x}_s + \hat{x}_l) \rangle$ and the difference of phase quadratures $\langle \delta^2(\hat{y}_s - \hat{y}_l) \rangle$ are smaller than the shot noise limit (SNL). The correlation variances depend on the squeezing parameter γ of the two-mode squeezed state [20, 21]:

$$\left\langle \delta^2(\hat{x}_s + \hat{x}_l) \right\rangle = \left\langle \delta^2(\hat{y}_s - \hat{y}_l) \right\rangle = 2e^{-2\gamma}. \tag{2}$$

γ is a positive real function of the noise frequency (Ω) with a value between zero and infinity. $\gamma = 0$, $\gamma > 0$ and $\gamma \to \infty$ correspond to no quantum correlation, partial correlation and perfect correlation, respectively. The schematic of the tripartite entangled state generation system from a NOPA is shown in figure 1 [10]. The two-mode squeezed state from NOPA is split by a beam-splitter of the transmission $T_1 = 2/3$ and the reflectivity $R_1 = 1/3$ consisting of a half-wave plate $(\lambda/2)$ and a polarizing-beam-splitter (PBS_1). Then the transmission beam is split

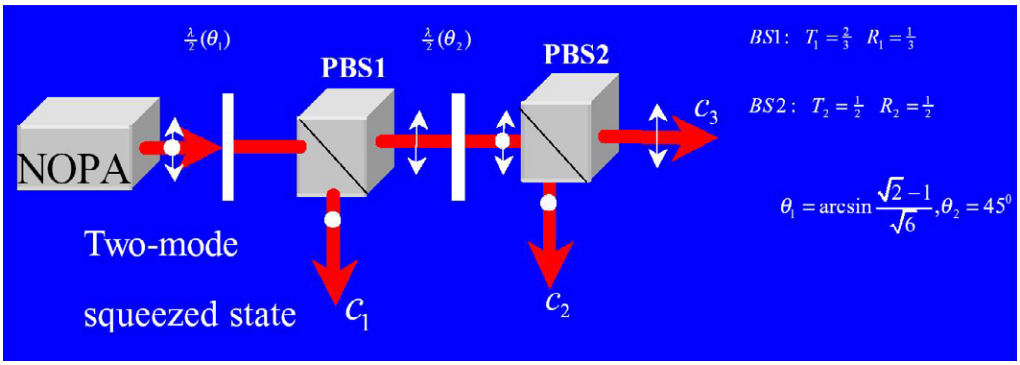

Figure 1. The schematic of the tripartite entangled state generation system.

again by a 50–50 ($T_2 = R_2 = 1/2$) beam-splitter ($\lambda/2$ and PBS_2) into two parts. The obtained optical modes $\hat{c}_1(\hat{x}_1, \hat{y}_1)$, $\hat{c}_2(\hat{x}_2, \hat{y}_2)$ and $\hat{c}_3(\hat{x}_3, \hat{y}_3)$ are in a tripartite squeezed state with both variances of the total amplitude quadratures of the three modes $\langle\delta^2(\hat{x}_1 + \hat{x}_2 + \hat{x}_3)\rangle$ and the relative phase quadratures of each pair-mode $\langle\delta^2(\hat{y}_k - \hat{y}_m)\rangle(k, m = 1, 2, 3, k \neq m)$, smaller than the corresponding shot noise limit (SNL). The measured original correlations between the signal and idler modes from the NOPA are about 4 dB below the SNL. After the correction to the electronic noise floor the noise reduction is -5.8 dB relative to the SNL and the corresponding squeezing parameter is $\gamma \approx 0.674$. The values of the left-sides of the inequalities for the inseparability criteria of the three modes are:

$$\begin{aligned}
&\text{I.} \quad \left\langle\delta^2(\hat{y}_1 - \hat{y}_2)\right\rangle + \left\langle\delta^2(\hat{x}_1 + \hat{x}_2 + \hat{x}_3)\right\rangle = 0.475 < 1,\\
&\text{II.} \quad \left\langle\delta^2(\hat{y}_2 - \hat{y}_3)\right\rangle + \left\langle\delta^2(\hat{x}_1 + \hat{x}_2 + \hat{x}_3)\right\rangle = 0.735 < 1,\\
&\text{III.} \quad \left\langle\delta^2(\hat{y}_1 - \hat{y}_3)\right\rangle + \left\langle\delta^2(\hat{x}_1 + \hat{x}_2 + \hat{x}_3)\right\rangle = 0.457 < 1,
\end{aligned} \tag{3}$$

here, we employed $g_i = 1$ for all i to make the verification simpler. If g_i are optimized to g_i^{opt} the values of correlation combination in the right-sides of equations (3) must be smaller. All correlation combinations are smaller than the normalized SNL and thus the modes $\hat{C}_1$, $\hat{C}_2$ and $\hat{C}_3$ are fully inseparable.

Furusawa's group in Tokyo obtained experimentally a cv tripartite entangled state with full inseparability by combining three independent squeezed vacuum states, which are generated from three subthreshold degenerate optical parametric oscillators (OPO) OPOl, OPO2 and OPO3, respectively, as shown in figure 2 [11]. A quadrature-phase squeezed state from OPO1 and two quadrature-amplitude squeezed states from OPO2 and OPO3, respectively are combined in a 'tritter' consisting of two beam-splitters with transmittance/reflectivity of 1/2 (BS1) and 1/1 (BS2). The measured average noise powers of the relative amplitude quadratures $\langle\delta^2(\hat{x}_1 - \hat{x}_2)\rangle$, $\langle\delta^2(\hat{x}_2 - \hat{x}_3)\rangle$ and $\langle\delta^2(\hat{x}_3 - \hat{x}_1)\rangle$, and that of the sum of all three phase quadratures $\langle\delta^2(\hat{y}_1 + \hat{y}_2 + \hat{y}_3)\rangle$ are 1.95, 2.04, 1.78 and 1.75 dB below the SNL, respectively, the corresponding values of the left-sides of the inequalities in equations (1) are about 0.851, 0.840 and 0.867, respectively ($g_i = 1$ for all three modes). In their experiment, three balanced homodyne detectors were employed and the full inseparability of cv among three optical modes was directly demonstrated.

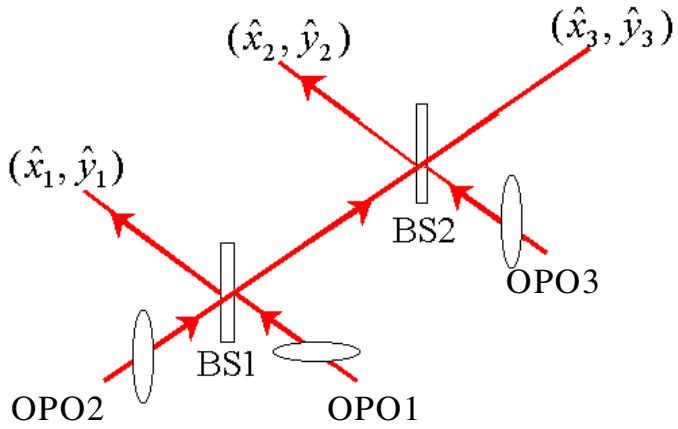

Figure 2. Schematic of tripartite entangled state generation by combining three independent squeezed vacuum states. OPO1–3: optical parametric oscillators 1–3, BS1: beam-splitter of 1 : 2 BS2: beam-splitter of 1 : 1.

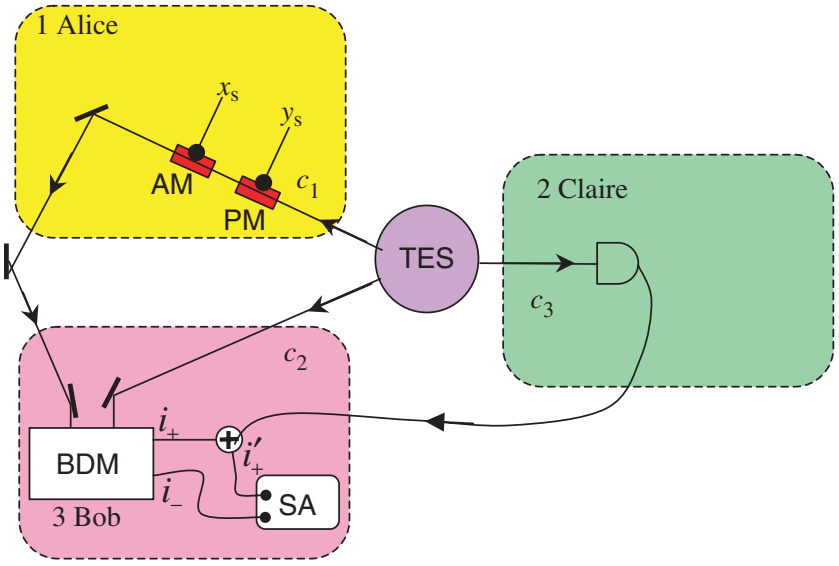

Figure 3. Schematic for controlled dense coding quantum communication.

3. Controlled dense coding quantum communication using tripartite entanglement of cvs

We theoretically proposed [19] and then experimentally realized [10] the controlled dense coding quantum communication network for cv using a tripartite entangled state of optical modes with directly detectable intensity. The three entangled modes $\hat{C}_1$, $\hat{C}_2$ and $\hat{C}_3$ are distributed to a sender (Alice), a receiver (Bob) and a controller (Claire), respectively (figure 3). The sender Alice modulates two sets of classical signals X_s and Y_s on the amplitude and phase quadratures of her mode $\hat{C}_1$ by the amplitude and phase modulators (AM and PM). The modulated signals X_s and Y_s at a given radio frequency (RF) can be considered as the

artificial noise added on the amplitude and phase quadratures, respectively. The modulated mode $\hat{C}_1'$ is sent to Bob who decodes simultaneously the modulated amplitude (X_s) and phase (Y_s) signals with the Bell-state direct measurement (BDM) equipment under the aid of his mode $\hat{C}_2$ [6, 22]. Taking into account the imperfect detection efficiency of the photodiodes ($\eta < 1$) and the nonzero losses of the optical system ($\xi_i < 1$), the noise power spectra of the sum and the difference photocurrents of $\hat{C}_1'$ and $\hat{C}_2$ modes are expressed by [10]:

$$\left\langle (\delta^2 i_+^2) \right\rangle = \langle \delta^2 (\hat{x}_{C_1'} + \hat{x}_{C_2}) \rangle = \eta^2 \xi_1^2 \frac{e^{2r} + 8e^{-2r} - 9}{12} + 1 + \frac{1}{2} V_{x_s}, \tag{4}$$

$$\left\langle (\delta^2 i_-^2) \right\rangle = \langle \delta^2 (\hat{y}_{C_1'} - \hat{y}_{C_2}) \rangle = 3\eta^2 \xi_1^2 \frac{e^{-2r} - 1}{12} + 1 + \frac{1}{2} V_{y_s}, \tag{5}$$

where V_{x_s} and V_{y_s} are the fluctuation variances of the modulated signals (x_s, y_s). The first term of equations (4) and (5) is the noise background formed by the quantum noise which affects the signal-to-noise ratio (SNR) of the measurement. When the squeezing parameter tends to infinity ($r \to \infty$), Bob only can measure the phase signal (equation (5)) with high SNR, however, he cannot gain the amplitude signal that is submerged in large noise background due to the presence of the antisqueezing noise term $e^{2\gamma}$ (equation (4)). The physical reason is that the modes $\hat{C}_1$, $\hat{C}_2$ and $\hat{C}_3$ construct a three-mode 'position' eigenstate with total amplitude quadrature $\langle \delta^2 (\hat{x}_{C_1} + \hat{x}_{C_2} + \hat{x}_{C_3}) \rangle \to 0$ and the relative phase quadratures $\langle \delta^2 (y_{C_k} - y_{C_m}) \rangle \to 0$ ($k \neq m$) in this case [8, 10]. For extracting the amplitude signal, Bob needs Claire's detecting result $\langle \delta^2 \hat{x}_{C_3} \rangle$ of the amplitude quadrature of mode $\hat{C}_3$ using a photodiode (D). If Claire sends the detected photocurrent $\hat{i}_3$ to Bob, Bob displaces Claire's result on $\hat{i}_+$ to generate a total photocurrent:

$$\hat{i}_+' = \hat{i}_+ + g\hat{i}_3, \tag{6}$$

where g describes the gain at Bob for the transformation from Claire's photocurrent to Bob's sum photocurrent. The calculations in [10, 19] pointed out that the optimal gain is $g_{\text{opt}} = \frac{1}{\sqrt{2}}$ for an ideal case of $\gamma \to \infty$, $\eta \to 1$ and $\xi \to 1$. For simplification, in our experiments the gain was adjusted to the value of $\frac{1}{\sqrt{2}}$ and the measured results were not affected severely although the conditions are not ideal. The variance of $\hat{i}_+'$ is equal to:

$$\langle \delta^2 \hat{i}_+' \rangle = \frac{1}{12} \left\{ e^{2r} \eta^2 \left[\frac{\xi_2^2 - \xi_1^2}{\xi_1} \right]^2 + 2e^{-2r} \eta^2 \left[\frac{\xi_2^2 - 2\xi_1^2}{\xi_1} \right]^2 \right.$$
$$\left. -3 \left[\frac{\xi_2^4}{\xi_1^2} \eta^2 - 4 + 3\eta^2 \xi_1^2 + 2\xi_2^2 \eta^2 - 2\frac{\xi_2^2}{\xi_1^2} \right] + \frac{1}{2} V_{X_s} \right\}. \tag{7}$$

The antisqueezing term ($e^{2\gamma}$) is significantly decreased and thus the SNR of X^s is improved. Especially, if $\xi_2 = \xi_1$, the large noise term will disappear. This means that Claire can control the information transmission capacity between Alice and Bob by sending or not sending the photocurrent $\hat{i}_3$ to Bob. The channel capacities without (C_{n-c}^{dense}) and with (C_c^{dense}) Claire's help deduced from equations (4), (5) and (7) are expressed in equations (8) and (9), respectively:

$$C_{n-c}^{\text{dense}} = \frac{1}{2} \ln \left[\left(1 + \frac{\sigma^2}{\langle \delta^2 \hat{i}_- \rangle} \right) \left(1 + \frac{\sigma^2}{\langle \delta^2 \hat{i}_+ \rangle} \right) \right], \tag{8}$$

$$C_c^{\text{dense}} = \frac{1}{2} \ln \left[\left(1 + \frac{\sigma^2}{\langle \delta^2 \hat{i}_- \rangle} \right) \left(1 + \frac{\sigma^2}{\langle \delta^2 i_+' \rangle} \right) \right], \tag{9}$$

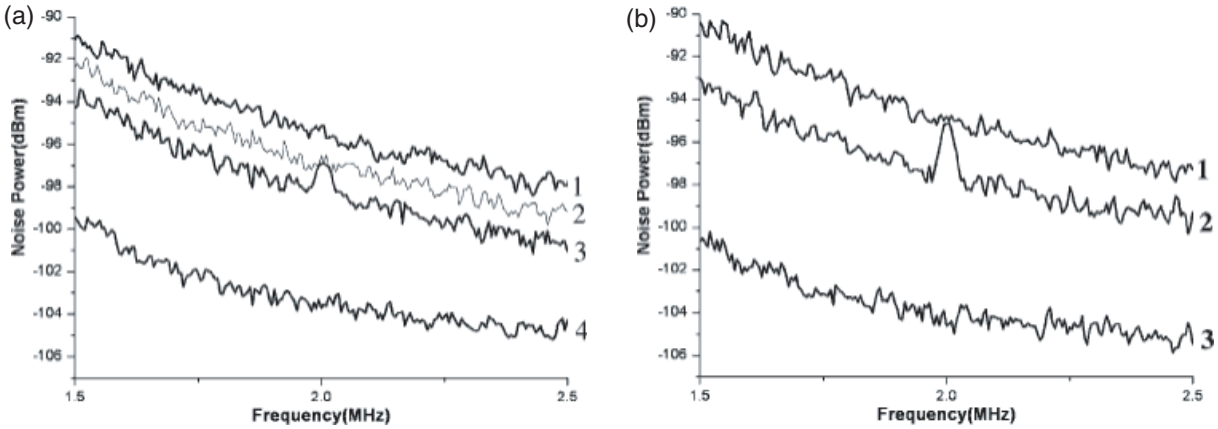

Figure 4. (a) The noise power spectra of amplitude sums $\langle\delta^2\hat{i}'_+\rangle$ (trace 3) and $\langle\delta^2\hat{i}_+\rangle$ (trace 2), trace 1-shot noise limit (SNL), trace 4—electronics noise level (ENL), measured frequency range 1.5–2.5 MHz, resolution bandwidth 30 KHz, video bandwidth 0.1 KHz. (b) The noise power spectra of phase difference $\langle\delta^2\hat{i}_-\rangle$ (trace 2), trace 1—SNL, trace 3—ENL, measured frequency range 1.5–2.5 MHz, resolution bandwidth 30 KHz, video bandwidth 0.1 KHz.

where σ^2 is the average value of the signal photon numbers. The photon numbers supplied to the communication system are used for the signal and squeezing. The total mean photon number ($\bar{n}$) involved in each optical mode is equal to [18]

$$\bar{n} = \sigma^2 + \sinh^2\gamma. \tag{10}$$

Figure 4 shows the power fluctuation spectra measured in our experiment. The traces 2 and 3 in figure 4(a) are the noise spectra for the amplitude sum photocurrents of two (trace 2 for $\langle\delta^2\hat{i}_+\rangle$) and three (trace 3 for $\langle\delta^2\hat{i}'_+\rangle$) optical modes, which are 1.0 and 2.7 dB below the SNL (trace 1), respectively. After the correction to the electronics noise floor, which is about 8 dB below the SNL (trace 4), the noise reductions of $\langle\delta^2\hat{i}_+\rangle$ and $\langle\delta^2\hat{i}'_+\rangle$ relative to the SNL should be actually 1.19 and 3.28 dB, respectively. Trace 2 in figure 4(b) is the measured noise power spectrum of $\langle\delta^2\hat{i}_-\rangle = \langle\delta^2(y_{c_1} - y_{c_1})\rangle$ for the relative phase-quadrature correlation between modes c_1 and c_2, which is 2.66 dB below the SNL (trace l). Accounting for the electronics noise (trace 3), it should actually be 3.18 dB below the SNL. Substituting the measured noise powers of $\langle\delta^2\hat{i}_+\rangle$, $\langle\delta^2\hat{i}'_+\rangle$ and $\langle\delta^2\hat{i}_-\rangle$ into equations (4)–(7), the squeezing parameter of $\gamma_{\rm exp} \approx 0.674$ is calculated. The dependences of the channel capacities with ($C_c^{\rm dense}$) and without ($C_{n-c}^{\rm dense}$) Claire's help on the mean photon number $\bar{n}$ are given in figure 5 according to the experimental parameters.

For comparison the channel capacity of an ideal single mode coherent state [$C^{\rm coh} = \ln(1+\bar{n})$] is also drawn in figure 5. We can see that, under the experimental conditions, the channel capacity with the help of Claire ($C_c^{\rm dense}$) is always larger than that without her help ($C_{n-c}^{\rm dense}$) which is the result of SNR improvement due to using three-partite entanglement. For example, when $\bar{n} = 11$, the channel capacity of the presented system can be controllably inverted between 2.91 and 3.14. The experiment shows that using the accessible entanglement of optical modes the channel capacity of the controlled dense coding quantum communication can exceed

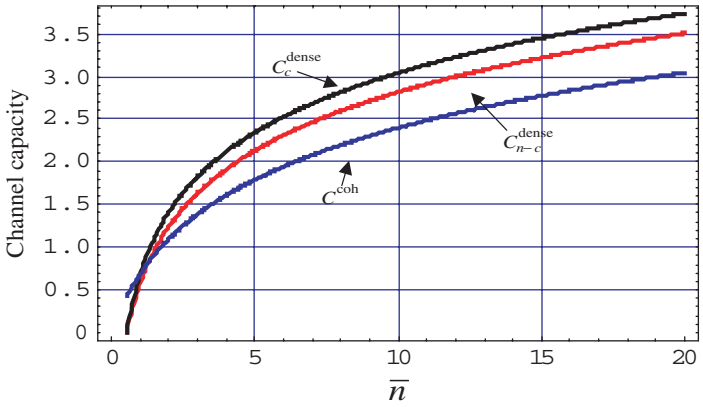

Figure 5. The dependences of the channel capacities on the mean photon number.

that of classical optical communication with a coherent state (C^{coh}) when the mean photon number $\bar{n}$ is larger than 1.00.

4. Quantum state secret sharing

Secret sharing is a powerful protocol for secure communication based on the interdependence among all shares. Blakely [23] and Shamir [24] proposed the scheme of the threshold secret sharing for classical information in 1979, which is to distribute a secret information to n shares firstly and to establish the interconnection among the n parties. In this construction, the secret information can be recovered only when k ($k \leqslant n$) shares collaborate and if the numbers of the collaborators are less than k the secret message cannot be extracted, this scheme was therefore named (k, n) threshold secret sharing. In quantum information science the shares of information are quantum states and the security of the communication can be enhanced using multipartite quantum entanglement distributed among these shares. Cleve *et al* [25] proposed the scheme of (k, n) threshold QSS for discrete states (qubits), in which the 'dealer' encodes a secret state into an n-party entangled state and distributes it to n 'players'. Any k players (the access structure) can collaborate to retrieve the quantum secret state, whereas the remaining $n-k$ players (the adversary structure), even when conspiring acquire nothing. Then Lance *et al* [26] theoretically proposed and experimentally demonstrated [27] (2, 3) threshold QSS utilizing tripartite cv entanglement. In their scheme, a secret coherent state was encoded into a tripartite entangled state and distributed to three players. The experimental results proved that any two of the three players can form an access structure to reconstruct the secret state. The state reconstruction was characterized in terms of fidelity, signal transfer and reconstructure noise.

The experimental schematic of (2, 3) QSS is shown in figure 6. The dealer combines two single-mode squeezed states ($\hat{a}_{\text{SQZ1}}$ and $\hat{a}_{\text{SQZ2}}$) produced from the two degenerate OPAs on a 1 : 1 beam-splitter (S_1) to generate a pair of EPR entangled beams ($\hat{a}_{\text{EPR1}}$ and $\hat{a}_{\text{EPR2}}$). Then, the dealer interferes beams $\hat{a}_{\text{EPR1}}$ and the secret state $\hat{a}_{\text{in}}$ on another 1 : 1 beam splitter (S_2). The two output fields from S_2 and the second entangled beam $\hat{a}_{\text{EPR2}}$ form a tripartite entangled state ($\hat{a}_1$, $\hat{a}_2$ and $\hat{a}_3$) which are distributed to player 1, player 2 and player 3. The dealer can further enhance the security of the scheme by displacing the coherent amplitudes of the shares with correlated Gaussian white noise [26]. Choosing the Gaussian noise to have the same correlations as the

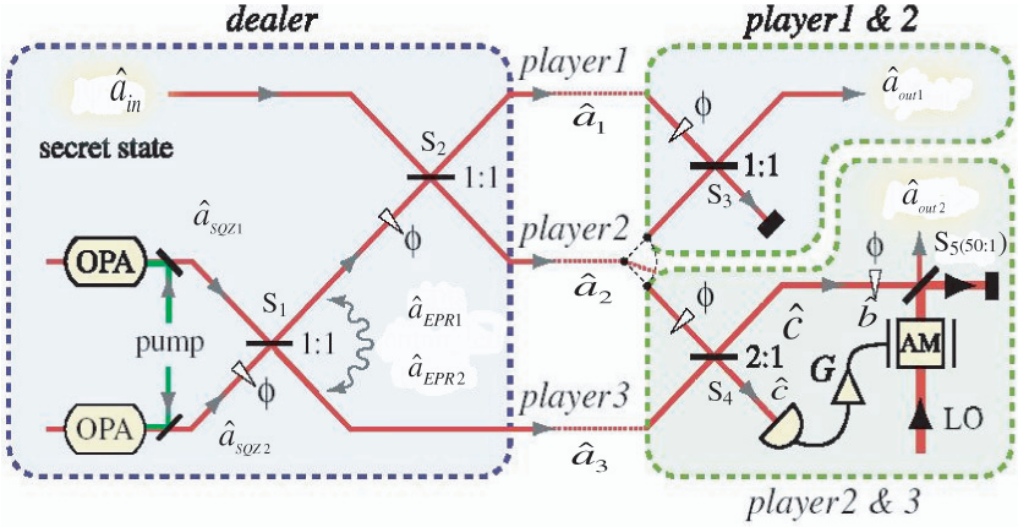

Figure 6. Schematic of the (2, 3) QSS scheme; $\hat{a}_{\rm in}$, input secret quantum state; OPA, optical parametric amplifier; G, electronic gain; AM, amplitude modulator; LO, optical local oscillator and S_{1-4}, beam-splitter.

quadrature entanglement, the shares can be expressed as

$$\hat{a}_1 = (\hat{a}_{\rm in} + \hat{a}_{\rm EPR1} + \delta N)/\sqrt{2}, \tag{11}$$

$$\hat{a}_2 = (\hat{a}_{\rm in} - \hat{a}_{\rm EPR1} - \delta N)/\sqrt{2}, \tag{12}$$

$$\hat{a}_3 = \hat{a}_{\rm EPR2} + \delta N^*, \tag{13}$$

where $\delta N = (\delta\hat{X}_N + {\rm i}\delta\hat{Y}_N)/2$ represents the Gaussian noise with mean $\delta\hat{X}_N = \delta\hat{Y}_N = 0$ and $\delta^2\hat{X}_N = \nu_{X_N}$, $\delta^2\hat{Y}_N = \nu_{Y_N}$, δN^* is the complex conjugate of $\delta\hat{N}$.

Combining modes $\hat{a}_1$ and $\hat{a}_2$ with a $1:1$ beam-splitter (S_3), the annihilation operator of the output field can be calculated with equations (11) and (12):

$$\hat{a}_{\rm out1} = \frac{\hat{a}_1 + \hat{a}_2}{\sqrt{2}} = \hat{a}_{\rm in}. \tag{14}$$

This means that players 1 and 2 (henceforth denoted by $\{1, 2\}$) only need to complete a Mach–Zehnder interferometer with use of a $1:1$ beam-splitter to retrieve the secret state. For the access structures $\{2, 3\}$ and $\{1, 3\}$, we can reconstruct the quantum state by utilizing a $2:1$ beam-splitter and an electro-optic feedforward loop [26]. As an example, we discuss the $\{2, 3\}$ access structure. The amplitude and phase quadratures of the output modes $\hat{b}$ and $\hat{c}$ from a $2:1$ beam-splitter (S_4) are expressed by [26]

$$\hat{X}_b = \frac{1}{\sqrt{3}}(\hat{Y}_{\rm SQZ2} - \hat{Y}_{\rm SQZ1} + \hat{X}_{\rm in} - 2\delta\hat{X}_N), \tag{15}$$

$$\hat{Y}_b = \frac{1}{\sqrt{3}}(\hat{X}_{\rm SQZ1} - \hat{X}_{\rm SQZ2} + \hat{Y}_{\rm in}), \tag{16}$$

$$\hat{X}_C = \frac{[(\hat{Y}_{\rm SQZ1} - \hat{Y}_{\rm SQZ2}) - 3(\hat{X}_{\rm SQZ1} + \hat{X}_{\rm SQZ2}) + 2(\hat{X}_{\rm in} + \delta\hat{X}_N)]}{\sqrt{24}} \tag{17}$$

$$\hat{Y}_C = \frac{[(\hat{X}_{\mathrm{SQZ1}} - \hat{X}_{\mathrm{SQZ2}}) - 3(\hat{Y}_{\mathrm{SQZ1}} + \hat{Y}_{\mathrm{SQZ2}}) + 2(\hat{Y}_{\mathrm{in}} - 3\delta\hat{Y}_N)]}{\sqrt{24}} \tag{18}$$

where, $\hat{X}_{\mathrm{SQZ1(2)}}$ and $\hat{Y}_{\mathrm{SQZ1(2)}}$ are the amplitude and phase quadrature of the squeezed state $\hat{a}_{\mathrm{SQZ1(2)}}$ from two OPAs. $\hat{X}_{\mathrm{in}}$ and $\hat{Y}_{\mathrm{in}}$ denote the amplitude and phase quadrature of the input secret state ($\hat{a}_{\mathrm{in}}$). For the ideal case with perfect squeezing the variance $\delta^2\hat{X}_{\mathrm{SQZ1(2)}}$ tends to zero. In this case, it is obvious from equation (16) that the phase quadrature $\hat{Y}_{\mathrm{in}}$ of $\hat{a}_{\mathrm{in}}$ is reconstructed in $\hat{Y}_b$ of mode $\hat{b}$. Comparing equations (15) and (17), we can see that if the amplitude noise of mode $\hat{c}$ is measured and then the measured photocurrent is fed back to mode $\hat{b}$ with an appropriate gain, the anti-squeezed noise ($\hat{Y}_{\mathrm{SQZ}}$) and the attached Gaussian white noise ($\delta\hat{X}_N$) can be eliminated. In the experiment of [27] the photocurrent δI of mode $\hat{c}$ was directly detected and the amplitude of a local light (LO) was modulated by δI. Then mode $\hat{b}$ was displaced by the modulated LO with a high reflecting beam-splitter S_5 (50 : 1) to reconstruct the amplitude quadrature of $\hat{a}_{\mathrm{in}}$ on the output mode $\hat{a}_{\mathrm{out2}}$. The measured photocurrent δI equals

$$\delta I = \sqrt{\eta}\langle\hat{X}_C\rangle\left\{\frac{1}{2}\sqrt{1/3}\sqrt{\eta}\left[\frac{1}{\sqrt{2}}(\delta\hat{Y}_{\mathrm{SQZ1}} - \delta\hat{Y}_{\mathrm{SQZ2}})\right]\right.$$
$$\left. -\frac{3}{\sqrt{2}}(\delta\hat{X}_{\mathrm{SQZ1}} + \delta\hat{X}_{\mathrm{SQZ2}}) + \sqrt{2}(\delta\hat{X}_N + \delta\hat{X}_{\mathrm{in}}) + \sqrt{1-\eta}\delta\hat{X}_d\right\}, \tag{19}$$

where η and $\delta\hat{X}_d$ are the efficiency of the detector (D) and the vacuum noise added due to imperfect detection, respectively. The amplitude and phase quadrature of mode $\hat{a}_{\mathrm{out2}}$ is

$$\hat{X}_{\mathrm{out2}}(\hat{Y}_{\mathrm{out2}}) = \sqrt{1-\varepsilon}\,\hat{X}_b(\hat{Y}_b) + \sqrt{\varepsilon}\,\hat{X}_{\mathrm{LO}}(\hat{Y}_{\mathrm{LO}}), \tag{20}$$

where ε denotes the reflectivity of S_5 ($\varepsilon = 1/50$ for this experiment), $\hat{X}_{\mathrm{LO}}$ and $\hat{Y}_{\mathrm{LO}}$ expresses the amplitude and phase quadrature of the LO, respectively. If $\varepsilon \to 0$, equation (20) becomes

$$\hat{X}_{\mathrm{out2}} \approx \hat{X}_b + k(\omega)\delta I,$$
$$\hat{Y}_{\mathrm{out2}} \approx \hat{Y}_b, \tag{21}$$

where $k(w)$ is the gain transformation function after accounting for the imperfect response of the feedback circuit and the optical loss of the beam-splitter S_5. Substituting equations (15), (16) and (19) into equations (21) the following expressions are obtained

$$\delta\hat{X}_{\mathrm{out2}} = \left(\frac{1}{\sqrt{3}} + \frac{G}{\sqrt{6}}\right)\delta\hat{X}_{\mathrm{in}} + \left(\frac{G}{2\sqrt{6}} - \frac{1}{\sqrt{3}}\right)(\delta\hat{Y}_{\mathrm{SQZ1}} - \delta\hat{Y}_{\mathrm{SQZ2}})$$
$$-\frac{G}{2}\sqrt{3/2}(\delta\hat{X}_{\mathrm{SQZ1}} + \delta\hat{X}_{\mathrm{SQZ2}}) + G\sqrt{\frac{1-\eta}{\eta}}\delta\hat{X}_d + \left(\frac{2}{\sqrt{3}} - \frac{G}{\sqrt{6}}\right)\delta\hat{X}_N \tag{22}$$

$$\delta\hat{Y}_{\mathrm{out2}} = \sqrt{\frac{1}{3}}\delta\hat{Y}_{\mathrm{in}} - \sqrt{\frac{1}{3}}(\delta\hat{X}_{\mathrm{SQZ1}} - \delta\hat{X}_{\mathrm{SQZ2}}), \tag{23}$$

where $G = \eta k(\omega)\langle\hat{X}_C\rangle$ is the total gain of the feedback circuit. If $G = 2\sqrt{2}$ is selected, the antisqueezed term ($\delta\hat{Y}_{\mathrm{SQZ}}$) and the attached noise ($\delta\hat{X}_N$) will be totally eliminated. For the ideal

limitation with perfect squeezing ($\delta\hat{X}_{\mathrm{SQZ}} \to 0$), we have

$$\delta\hat{X}_{\mathrm{out2}} = \sqrt{3}\delta\hat{X}_{\mathrm{in}},$$
$$\delta\hat{Y}_{\mathrm{out2}} = \frac{1}{\sqrt{3}}\delta\hat{Y}_{\mathrm{in}}. \tag{24}$$

Thus, {2, 3} QSS can reconstruct the transformation of the input secret quantum state ($\hat{a}_{\mathrm{in}}$). Since the transformation is a local unitary operation the quantum information of the input state will not be lost. With a similar scheme the {1, 3} QSS can also be completed.

The overlap between the input secret and reconstructed quantum state is expressed with the fidelity $F = \langle a_{\mathrm{in}}|\rho_{\mathrm{out}}|a_{\mathrm{in}}\rangle$, thus the quality of the state reconstruction for the access and adversary structures in QSS can be measured by the fidelity, usually [28]. Assuming that all fields involved have Gaussian statistics and that the input state is a coherent state, the fidelity can be expressed in terms of experimentally measurable parameters as

$$F = 2\mathrm{e}^{-(K^+ + K^-)/4}/\sqrt{(1+\langle\delta^2\hat{X}_{\mathrm{out}}\rangle)(1+\langle\delta^2\hat{Y}_{\mathrm{out}}\rangle)}, \tag{25}$$

where $K^+ = \langle\hat{X}_{\mathrm{in}}\rangle^2(1-g^+)^2/(1+\langle\delta^2\hat{X}_{\mathrm{out}}\rangle)$, $K^- = \langle\hat{Y}_{\mathrm{in}}\rangle^2(1-g^-)^2/(1+\langle\delta^2\hat{Y}_{\mathrm{out}}\rangle)$, $g^+ = \langle\hat{X}_{\mathrm{out}}\rangle/\langle\hat{X}_{\mathrm{in}}\rangle$ and $g^- = \langle\hat{Y}_{\mathrm{out}}\rangle/\langle\hat{Y}_{\mathrm{in}}\rangle$ are the gains of amplitude and phase quadratures, respectively. In the experiment with figure 6, the fidelity for {1, 2} can be determined directly. However, for {2, 3} and {1, 3} the fidelity is determined by inferring the unitary parametric operation

$$\delta\hat{X}_{\mathrm{para}} = \frac{1}{\sqrt{3}}\delta\hat{X}_{\mathrm{out}},$$
$$\delta\hat{Y}_{\mathrm{para}} = \sqrt{3}\delta\hat{Y}_{\mathrm{out}}, \tag{26}$$

on the reconstructed state, so in the ideal case we have $\delta\hat{X}_{\mathrm{para}} = \delta\hat{X}_{\mathrm{in}}$ and $\delta\hat{Y}_{\mathrm{para}} = \delta\hat{Y}_{\mathrm{in}}$ (see equations (24)). This means that the input state is perfectly reconstructed. When the protocol is operating at unitary gain, under ideal conditions any one of the access structures can achieve $F = 1$ corresponding to perfect reconstruction of the input secret quantum state, whilst the corresponding adversary structure obtains $F = 0$.

In the experiment of [27] the two OPA were pumped by green light at 532 nm which was the output second harmonic wave from a CW Nd : YAG frequency doubled laser. The output fundamental wave at 1064 nm served as a coherent field to provide a shared time frame (universal local oscillator) between all parties, to yield the dealer secret by displacing the sideband vacuum state of the laser field using an amplitude and a phase modulator at 6.12 MHz, and to produce two amplitude squeezed states from hemilithic MgO : $LiNbO_3$ OPAs pumped with 532 nm light. The output fields of each OPA were squeezed at 4.5 ± 0.2 dB below the quantum noise limit. The two squeezed light beams were interfered on a 1 : 1 beam-splitter (S_1) with an observed visibility of $99.2 \pm 0.2\%$ and a controlled relative phase of $\pi/2$. The beam-splitter outputs were EPR entangled which satisfied the wavefunction inseparability criterion [9]. The measured correlation product was

$$\frac{1}{4}\left[\langle(\delta\hat{X}_{\mathrm{EPR1}} + \delta\hat{X}_{\mathrm{EPR2}})^2\rangle \cdot \langle(\delta\hat{Y}_{\mathrm{EPR1}} - \delta\hat{Y}_{\mathrm{EPR2}})^2\rangle\right] = 0.44 \pm 0.02 < 1. \tag{27}$$

In order to enhance the security of the secret state against the adversaries, the coherent quadrature amplitudes of the entangled beams are displaced with Gaussian noise. The variance

of this noise was characterized to be $V_N = 3.5 \pm 0.1$ dB normalized to the quantum noise limit. A homodyne detector was used to characterize the secret, adversary and reconstructed quantum states using a configuration of removable mirrors. The total homodyne detection efficiency, $\eta_{\text{hom}} = 0.89 \pm 0.01$, is inferred out of each measurement. The fidelities can be calculated from these measured variances of the amplitude and phase quadratures [27]. The fidelity obtained from the noise spectra was $F_{\{1,2\}} = 0.93 \pm 0.02$ with optical quadrature gains of $g^+ = 0.94 \pm 0.01$ and $g^- = 0.97 \pm 0.01$, respectively. The corresponding adversary $\{3\}$ structure had a fidelity of $F_{\{3\}} = 0$ since their share contained no component of the input secret state. The measured fidelity at the unitary gain point for the $\{2, 3\}$ protocol was $F_{\{2,3\}} = 0.63 \pm 0.01$ with $g^+ g^- = (1.77 \pm 0.01)(0.58 \pm 0.01) = 1.02 \pm 0.01$. The corresponding adversary structure $\{1\}$ achieves a fidelity of only $F_{\{1\}} = 0.03 \pm 0.01$. The quantum nature of this experiment was demonstrated by the fidelity averaged over all the access structures $F_{\text{avg}}^{\text{clas}} = 0.74 \pm 0.04$, which exceeded the classical limit $F_{\text{avg}}^{\text{clas}} = 2/3$. Without entanglement the maximum fidelity achievable by $\{2, 3\}$ and $\{1, 3\}$ is $F_{\{2,3\}}^{\text{clas}} = F_{\{1,3\}}^{\text{clas}} = 1/2$ whilst $\{1, 2\}$ can still achieve $F_{\{1,2\}}^{\text{clas}} = 1$, so the average fidelity achieved by all permutations of the access structure cannot exceed $F_{\text{avg}}^{\text{clas}} = 2/3$. This defines the classical boundary for $\{2, 3\}$ threshold QSS. For a general $\{k, n\}$ threshold QSS scheme, independent of the dealer protocol, the maximum average classical fidelity achievable without entanglement resources is $F_{\text{avg}}^{\text{clas}} = k/n$. If F_{avg} exceeds k/n, quantum resources must be utilized and thus the communication protocol is in the quantum information realm.

5. Prospection

Multipartite entanglement shared by more than two parties is a subtle issue and also a necessary resource for achieving quantum communication networks and quantum computation. The quantification of multipartite entanglement of more than three parties in Gaussian states was theoretically analyzed and the experimental accessibility with the optimal fidelity of cv teleportation networks was discussed recently [29]. A nice review article on multipartite entanglement for cv systems, which is more focused on theoretical aspects [30], is a good complement to the present paper. The quadripartite cluster and GHZ entangled states for cvs have been experimentally prepared by our group [31]. Menicucci *et al* [32] theoretically proved that the universal quantum computation can be achieved with cv cluster states as long as a non-Gaussian measurement can be performed. The multipartite entanglement of cvs provides rich and valuable resources for quantum information. The quantum optical implementations based upon cvs offer us an efficient approach to demonstrate experimentally the general principles of quantum information science and technology.

Acknowledgments

This work was supported by the National Science Foundation of China (grant no. 10674088, 60608012 and 60736040) and PCSIRT (grant no. IRT0516).

References

[1] Coffiman V, Kundu J and Wootters W K 2000 *Phys. Rev.* A **61** 052306
[2] Adesso G and Illuminati F 2006 *New J. Phys.* **8** 15

[3] Adesso G, Serafini A and Illuminati F 2006 *Phys. Rev.* A **73** 032345
[4] Braunstein S and van Loock P 2005 *Rev. Mod. Phys.* **77** 513
[5] Furusawa A, Sorensen J L, Braunstein S L, Fuchs C A, Kimble H J and Polzik E S 1998 *Science* **282** 706
[6] Li X Y, Pan Q, Jing J T, Zhang J, Xie C D and Peng K C 2002 *Phys. Rev. Lett.* **88** 047904
[7] Jia X J, Su X L, Pan Q, Gao J R, Xie C D and Peng K C 2004 *Phys. Rev. Lett.* **93** 250503
[8] van Loock P and Braunstein S L 2000 *Phys. Rev. Lett.* **84** 3482
[9] van Loock P and Furusawa A 2003 *Phys. Rev.* A **67** 052315
[10] Jing J T, Zhang J, Yan Y, Zhao F G, Xie C D and Peng K C 2003 *Phys. Rev. Lett.* **90** 167903
[11] Aoki T, Takei N, Yonezawa H, Wakui K, Hiraoka T and Furusawa A 2003 *Phys. Rev. Lett.* **91** 080404
[12] Lance A M, Symul T, Bowen W P, Sanders B C and Lam P K 2004 *Phys. Rev. Lett.* **92** 177903
[13] Yonezawa H, Aoki T and Furusawa A 2004 *Nature* **431** 430
[14] Adesso G and Illuminati F 2005 *Phys. Rev. Lett.* **95** 150503
[15] Adesso G, Serafini A and Illuminati F 2007 *New J. Phys.* **9** 60
[16] Audenert K, Verstraete F and Moor B D 2001 *Phys. Rev.* A **64** 052304
[17] van Loock P and Braunstein S L 2001 *Phys. Rev.* A **63** 022106
[18] Greenberger D M, Horne M A, Shimony A and Zeilinger A 1990 *Am. J. Phys.* **58** 1131
[19] Zhang J, Xie C D and Peng K C 2002 *Phys. Rev.* A **66** 032318
[20] Reid M D 1989 *Phys. Rev.* A **40** 913
[21] Zhang Y, Su H, Xie C D and Peng K C 1999 *Phys. Lett.* A **259** 171
[22] Zhang J and Peng K C 2000 *Phys. Rev.* A **62** 064302
[23] Blakely G 1979 *Proceedings of the National Computer Conference (New York)* vol 48 (Montrale, NJ: AFIPS) pp 313–17
[24] Shamir A 1979 *Commun. ACM* **22** 612
[25] Cleve R, Gottesman D and Lo H K 1999 *Phys. Rev. Lett.* **83** 648
[26] Lance A M, Symul T, Bowen W P, Tyc T, Sanders B C and Lam P K 2003 *New J. Phys* **5** 4
[27] Lance A M, Symul T, Bowen W P, Sanders B C and Lam P K 2004 *Phys. Rev. Lett.* **92** 177903
[28] Schumacher B 1995 *Phys. Rev.* A **51** 2738
[29] Adesso G and Illuminati F 2007 *Preprint* quant-ph/0703277
[30] Adesso G and Illuminati F 2007 *Preprint* quant-ph/0701221
[31] Su X L, Tan A H, Jia X J, Zhang J, Xie C D and Peng K C 2007 *Phys. Rev. Lett.* **98** 070502
[32] Menicucci N C, van Loock P, Gu M, Weedbrook C, Ralph T C and Nielsen M A 2006 *Phys. Rev. Lett.* **97** 110501